2013 European Control Conference (ECC)
July 17-19, 2013, Zürich, Switzerland.

# Fractional Order PD$^{\mu}$ Control of a Visual Servoing Manipulator System

Cosmin Copot[1], Clara M. Ionescu[1], Corneliu Lazar[2] and Robin De Keyser[1]

*Abstract*— **In this paper, a fractional order PD$^{\mu}$ controller based on visual features is presented. A manipulator robot with 6 degrees of freedom and an eye-in-hand camera configuration is employed to design a visual servoing control architecture. The image based control law was designed using point features. A Matlab simulator which implements the visual control architecture was developed and the results were compared with a classical integer order controller. The validity of the visual based controllers is shown by the simulation results which demonstrate that the proposed approach based on a fractional order controller has a stable and convergent behavior when dealing with visual servoing applications. The fractional order PD$^{\mu}$ controller provides better performances in comparison with an integer order PD controller.**

## I. INTRODUCTION

The robot motion tracking systems represent one of the most challenging control applications in the field of manipulator robots due to the highly non-linear and time varying dynamics. Numerous control algorithms have been proposed to deal with nonlinear dynamics of manipulator robots [1], [2], [3]. Hitherto, many types of control schemes have been proposed to control manipulator robots [4]. In recent years, many studies and applications of fractional order systems in areas as science and engineering have been presented, but there is still much room for developing this emerging tools. In this paper, we focus on the Fractional Order Proportional-Derivative (FOPD) controller performances in dealing with the nonlinear dynamics of a manipulator system. Recently, fractional order control of nonlinear systems has started to attract the interest for applications in control engineering [5], [6].

Image based visual servoing (IBVS) is an important technique used for solving the complex problems of controlling robot systems. An image based-controller can be designed not only using a proportional control law, but also with advanced control techniques which imply the knowledge of an open-loop model of the visual servo control system. In [7] a linear approximation around the working points of a multivariable controller was used to control a fast visual servo system of a two links arm. The robot is modelled taking into account the flexibility in the link and the dynamics of the velocity controlled actuators. The proposed model was used to design a GPC controller, and also an advanced controller in the frequency domain ($H_{\infty}$ controller). In [8], Hashimoto assumes that the robot dynamic is modelled as a perfect Cartesian motion device and uses point features, in order to control a 6 d.o.f robot with a LQ state feedback controller. The visual servoing system presented in [9] considered an ARIMAX multivariable model for the manipulator robot, which allows the implementation of a GPC controller. Another approach in modelling the robot is the Virtual Cartesian Motion Device (VCMD) described in [10].

Another model of a visual servo system is given in [11] and it employs camera position controller with a robust disturbance observer in the joint space. In this way each joint axis is decoupled and the inner loop can be expressed in the frequency region below the cut-off frequency of the robust disturbance observers as a diagonal transfer matrix. In [12], the IBVS structures based on nonlinear model predictive control are used for controlling manipulators with catadioptric cameras. Also, for a 3D visual servoing task, a nonlinear predictive approach is presented in [13]. An interesting approach for image based visual servoing is by using nonlinear model predictive control (NMPC) [14]. The relation between the variation of the visual features in image plane and the camera velocity vector in Cartesian space is done using a nonlinear operator named usually interaction matrix. Considering the complexity of visual servoing tasks, advanced control techniques are needed, in order to design stable and robust image based controllers.

In this paper, the application of fractional order control for a visual servoing system was studied. The designed control architecture consists of a 6 d.o.f. manipulator robot with a visual sensor mounted on the last robot arm. Visual information, as point features, acquired from a sensor are used in the fractional order controller to steer a robot from an initial to a desired configuration. The proposed architecture was implemented, tested and validated using a simulator developed by the authors in Matlab. The simulation results revealed good performances and show a stable and convergent behavior of the servoing system when dealing with image based fractional order control law. A comparison with a classical proportional controller was conducted and experimental results were revealed.

The paper is structured as follows: in Section II, the principle of an image based control architecture and an analytical method for computing the interaction matrix are presented. Section III is devoted to the fractional order control algorithm. The experimental results are presented in Section IV and the conclusions are detailed in the last Section.

[1]C. Copot, C.M. Ionescu and R. De Keyser are with Department of Electrical energy, Systems and Automation, Technologiepark 913, 9052, Ghent University, Belgium, {cosmin.copot, claramihaela.ionescu, robain.dekeyser} at ugent.be

C.M. Ionescu is a post-doc fellow of the Research Foundation-Flanders (FWO).

[2]C. Lazar is with the Department of Automatic Control and Applied Informatics, Dimitrie Mangeron 27, 700050, Technical University of Iasi, Romania, clazar at ac.tuiasi.ro

## II. PRINCIPLES OF A VISUAL SERVOING SYSTEM

### A. Visual features

Controlling a robot system using visual information acquired by a camera is the main goal of any IBVS control architecture. A schematic overview is given in Fig.1. The considered robot system is a 6 d.of. manipulator robot that has a visual sensor mounted on its last joint (eye-in-hand configuration). The open loop model of the visual servoing system from Fig.1 consists of two models: i) the robot model considered most of the times as a VCMD and ii) the visual sensor. The first one has as the input the reference camera velocity $\mathbf{v}_c^*$ and generates the camera velocity screw $\mathbf{v}_c$ depending on the robot dynamics. Typically, the visual sensor is composed of a camera and an image processing block used to extract point features from the image.

In order to achieve the main objective of IBVS, a trajectory for the video camera must be designed. The trajectory is given through the integration of the camera velocity obtained from the IBVS architecture by minimizing the error between the current visual features configuration and the desired one. In our approach we consider that the object is characterized by $n$ point features of coordinates $(u_i, v_i), i = \overline{1,n}$ defined by:

$$f = [f_1^T ... f_n^T]. \tag{1}$$

The error between point features in the image plane is:

$$e(k) = f(k) - f^*, \tag{2}$$

where $f(k)$ represents the point features configuration at the iteration $k$, while $f^*$ is the desired vector configuration. Equation (2) is the general representation of the input signal for the image based controller. The outputs of the image based controller is $\mathbf{v}_c^*$ of the camera. Once the task of extracting point features is completed then a relationship between time variation of $f(k)$ and camera velocity can be generated. Let $\mathbf{v}_c = [v, \omega]$ be the camera velocity vector with $v = [v_x, v_y, v_z]$ and $\omega = [\omega_x, \omega_y, \omega_z]$ the linear, respectively, angular velocity components.

Considering that the point features are defined relative to the camera frame, the time variation of $f$ can be computed with respect to the camera velocity by:

$$\dot{f} = \frac{\partial f}{\partial \mathbf{r}} \dot{\mathbf{r}} + \frac{\partial f}{\partial t}, \tag{3}$$

where $\mathbf{r}(t)$ represent the relationship between the camera frame and the object frame at the moment $t$. Next, we consider that the object is static ($\frac{\partial f}{\partial t} = 0$). Starting from the fundamental cinematic equation, the velocity of a 3D point related to the camera velocity can be computed by:

$$\dot{\mathbf{X}} = -v - \omega \times \mathbf{X} = -v + [\mathbf{X}]_\times \omega, \tag{4}$$

where $[\mathbf{X}]_\times$ is the antisymmetric matrix for $\mathbf{X}$. Combining (3) with (4) and using the perspective projection from 3D space in 2D space, the relationship between the motion of point features ($\dot{f}$) and camera velocity ($\mathbf{v}_c$) can be defined as [4]:

$$\dot{f} = L_f \mathbf{v}_c, \tag{5}$$

where by $L_f \in \mathbb{R}^{2n \times 6}$ is denoted the interaction matrix of the $n$ point features that compose the vector $f$. From (2) and (5) the connection between time variation of the error and camera velocity can be easily computed by:

$$\dot{e} = L_f \mathbf{v}_c. \tag{6}$$

Most of the visual servoing systems implementation do not take into account the dynamics of the robot and thus $\mathbf{v}_c = \mathbf{v}_c^*$. If an exponential decoupled decrease of the error is desired, a **classical proportional control** law is defined by:

$$\mathbf{v}_c^* = -\lambda L_f^+ e, \tag{7}$$

where $L_f^+ \in \mathbb{R}^{6 \times 2n}$ is the Moore-Penrose pseudoinverse of $L_f$, that is $L_f^+ = (L_f^T L_f)^{-1} L_f^T$. The interaction matrix for a point feature can be computed using [15]:

$$L_f^1 = \begin{bmatrix} -\frac{1}{z} & 0 & \frac{x}{z} & xy & -(1+y^2) & y \\ 0 & \frac{1}{z} & \frac{y}{z} & 1+y^2 & -xy & -x \end{bmatrix}, \tag{8}$$

where $z$ is the depth of the corresponding projection point in the Cartesian space related to the camera frame. The interaction matrix of detected point features is defined as:

$$L_f = [L_{f1} ... L_{fn}]^T. \tag{9}$$

The presented scheme consists of a VCMD, a Visual Sensor (VS) and the Image based Controller (IbC). In Fig. 1 it can be observed that as input the VCMD has the reference camera velocity denoted $\mathbf{v_c}^*$ and as output the camera velocity screw $\mathbf{v}_c$. The Visual Sensor has as input $\mathbf{v}_c$ and generates the vector $f(k) = (u_i(k), v_i(k)), i = \overline{1,n}$ that stores the coordinates of the visual features from the image.

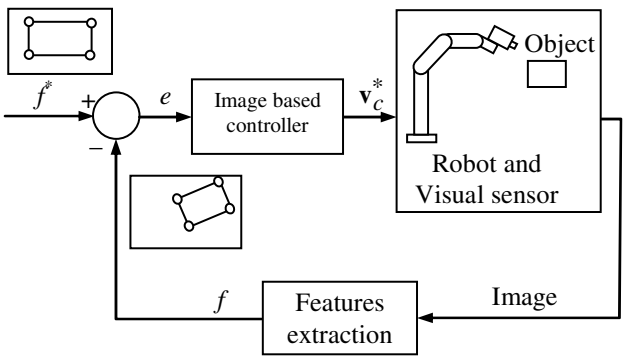


Fig. 1. Visual servoing closed loop architecture

### B. Plant model

The plant for this study is composed of a 6 d.o.f manipulator (representing the VCMD) and an eye in hand camera (VS). The VCMD is considered an inner velocity loop which controls the camera velocity and the outer one implements the image based control loop. The inner loop is regarded as an analog system because the sampling period of the

inner loop is very small (usually 1 ms) and it is described by a transfer matrix. This transfer matrix approximates the nonlinear robot dynamics using different approaches [9], [11] and typically has a diagonal form obtained through a suitable design of the multivariable inner velocity control loop. The input of the VCMD is the camera velocity reference which is applied to analog velocity control loops described by the transfer matrix through a zero-order hold (ZOH).

*1) Virtual Cartesian Motion Device Model:* Let $[t_1 \quad t_2 \quad t_3 \quad t_4 \quad t_5 \quad t_6]^T$ be the transformation that converts a homogeneous matrix into 6 Cartesian space then the robot Jacobian is defined by:

$$J_r = \begin{bmatrix} \frac{\partial t_1}{\partial q_1} & \cdots & \frac{\partial t_1}{\partial q_6} \\ \vdots & \ddots & \vdots \\ \frac{\partial t_6}{\partial q_1} & \cdots & \frac{\partial t_6}{\partial q_6} \end{bmatrix}, \tag{10}$$

where $q_i, \quad i = \overline{1,6}$ represent the state of the robot joints. One way to achieve a decoupled system is to employ a robust control strategy based on the joint space disturbance observer (DOB) and thus each joint axis is considered decoupled under the cut-off frequency of DOB [11]. The velocity controller is considered as a diagonal gain matrix:

$$\mathbf{K}_v = diag\{k_v, k_v, ..., k_v\}. \tag{11}$$

If the non-singularity of the robot Jacobian $J_r$ in the camera coordinates is assured, the transfer function from the acceleration command $\dot{\mathbf{v}}_c$ to the velocity $\mathbf{v}_c$ can be considered as a integrator system in the frequency region below the cut-off frequency.

The typical sampling period of the VCMD system is 0.2-1 $ms$ and the typical cut-off frequency is 150-300 $rad/s$. Since the velocity controller is usually a proportional one with an amplification value $k_v$, the inner loop system can be expressed in the frequency region below the cut-off frequency as:

$$\mathbf{v}_c(s) = G(s)\mathbf{v}_c^*(s) = \frac{k_v}{s + k_v} I_6 \mathbf{v}_c^*(s), \tag{12}$$

where $I_6$ is the identity matrix. Thus the following linearized discrete model for VCMD is obtained:

$$G(z^{-1}) = (1 - z^{-1}) Z\left(G(s)/s\right), \tag{13}$$

where $Z$ symbolizes $z$ transform. Using the VCMD model, the visual control law from (7) becomes:

$$\mathbf{v}_c^* = -\lambda G^{-1}(z^{-1}) L_f^+ e. \tag{14}$$

*2) Visual Sensor Model:* Typically, the visual sensor is composed of a camera and an image processing block used to extract the features from the image. Considering the poses of the camera and object be $x_c \in \mathbb{R}^6$ and $x_0 \in \mathbb{R}^6$, the camera is modeled by the mapping:

$$\beta : \mathbb{R}^6 \times \mathbb{R}^6 \to \mathbb{R}^{2n} \tag{15}$$

where *n* point features are selected to characterize the object.

The camera is modeled using the mapping (15) as a function of $x_c$ and $x_0$. The image processing block is modeled as:

$$f = g\left(\beta(x_c, x_o)\right), \tag{16}$$

where $g$ is a function that models the feature extracting algorithms.

In order to get the visual sensor model, there are firstly considered the frames attached to the robot base $F_b$, to the camera $F_c$ and to the object $F_o$. Let $T_c^b$ and $T_o^b$ be the homogeneous transformations between the frames $F_c$ and $F_b$ and, respectively, $F_o$ and $F_b$. It is assumed that the object feature positions $\mathbf{x}_o^b$ related to the frame $F_b$ is known and that the desired features $f^*$ were extracted using a suitable operator. The homogeneous transformation $T_c^b(0)$ for the camera start position is also considered known.

In order to obtain the homogeneous transformation $T_c^b(k)$, the camera velocity $\mathbf{v}_c(k)$ is integrated. The following homogeneous matrix is obtained:

$$T_c^b(k) = \begin{bmatrix} \mathbf{R}_{RPY}(k) & \mathbf{t}(k) \\ 0 & 1 \end{bmatrix}, \tag{17}$$

where:

$$\mathbf{R}_{RPY} = \begin{bmatrix} c_\varphi c_\vartheta & c_\varphi s_\vartheta s_\psi - s_\varphi c_\psi & c_\varphi s_\vartheta c_\psi + s_\varphi s_\psi \\ s_\varphi c_\vartheta & s_\varphi s_\vartheta s_\psi + c_\varphi c_\psi & s_\varphi s_\vartheta c_\psi - c_\varphi s_\psi \\ -s_\vartheta & c_\vartheta s_\psi & c_\vartheta c_\psi \end{bmatrix} \tag{18}$$

is the rotation matrix expressed using the roll, pitch and yaw approach, and $\mathbf{t}(k)$ is the translation vector. The $c_{(.)}$ and $s_{(.)}$ notations represent the *cosinus* and *sinus* functions. Computing the inverse of $T_c^b(k)$, the homogeneous transformation $T_b^c(k)$ is derived and multiplying it with the object feature position $\mathbf{x}_o^b$ related to the frame $F_b$, the object feature position $\mathbf{x}_f^c$ related to camera frame $F_c$ is got. Having the feature position $\mathbf{x}_f^c = [x_i, y_i, z_i]^T$, the intrinsic camera parameters $p_x$, $p_y$ and the image center point coordinates $(u_0, v_0)$, the point features coordinates expressed in pixels are obtained based on the perspective projection:

$$u_i = \frac{x_i}{z_i} p_x + u_0; \quad v_i = \frac{y_i}{z_i} p_y + v_0. \tag{19}$$

The Visual Sensor model represented by (15) - (19) has as input the camera velocity $\mathbf{v}_c(k)$ and as output the point feature coordinates stored in $f(k)$.

## III. Fractional order controller

In this section, a fractional order PD$^\mu$ algorithm for a visual servoing manipulator system is presented. The PD$^\mu$ controller has the following form of transfer function:

$$C_i(s) = K_{p_i}(1 + K_{d_i} s^{\mu_i}), \mu \in (0, 1], i = \overline{1,6}, \tag{20}$$

where $K_{p_i}$ and $K_{d_i}$ represent the proportional and derivative gains, and $\mu_i$ is the fractional order, for joint $i$.

The fractional differential equations can be specified in terms of the general fundamental operator ${}_aD_t^\mu$ as a generalization of the integration and differentiation operator, where $\mu$ is the fractional order and $a, t$ are limits which represent the initial conditions [16]. The most commonly

used definitions are the Riemann-Liouville (RL) and the Grunwald-Letnikov (GL). The RL definition of the fractional derivative of the signal $\rho$ is given by:

$$ {}_aD_t^{\mu}\rho(t) = \frac{1}{\Gamma(n-\mu)}\frac{d^n}{dt^n}\int_a^t (t-\tau)^{n-\mu-1}\rho(\tau)d\tau, \quad (21) $$

where $\Gamma$ is the gamma function defined by:

$$ \Gamma(x) = \int_0^{\infty} e^{-t}t^{x-1}dt. \quad (22) $$

The GL definition, which is the case of interest here, has the following form:

$$ {}_aD_t^{\mu}\rho(t) = \lim_{h\to 0}\frac{1}{h^{\mu}}\sum_{j=0}^{[(t-\mu)/h]}(-1)^j\begin{pmatrix}\mu\\ j\end{pmatrix}\rho(t-jh), \quad (23) $$

where $[\cdot]$ gives the integer part of its argument.

The fractional order proportional derivative controller defined by (20) can be written as:

$$ C_i(j\omega) = K_{p_i}\left(1 + K_{d_i}\omega^{\mu_i}\cos\frac{\mu_i\pi}{2} + jK_{d_i}\omega^{\mu_i}\sin\frac{\mu_i\pi}{2}\right). \quad (24) $$

In order to design the fractional controller, we assume that $L$ with $L^{*+}$ compensate each other and thus $LL^{*+} \approx I_{2n\times 2n}$. In this context the process can be defined as:

$$ P(s) = \frac{1}{s}G(s) = diag\{P_i(s)\}. \quad (25) $$

From the basic definition of the gain crossover frequency $\omega_{cg}$ and the phase margin $\varphi_m$, the next specification [16] has to be met by the fractional order controller:

$$ \varphi_m = arg[C_i(j\omega_{cg})P_i(j\omega_{cg})] + \pi. \quad (26) $$

Thus, the phase is given by:

$$ arg[C_i(j\omega)P_i(j\omega)]\,|_{\omega=\omega_{cg}} = \tan^{-1}\frac{\sin\frac{(1-\mu_i)\pi}{2} + K_{d_i}\omega_{cg}^{\mu_i}}{\cos\frac{(1-\mu_i)\pi}{2}} + \frac{\mu_i\pi}{2} - \pi - \tan^{-1}(\omega_{cg}\tau), \quad (27) $$

where $\tau$ is the time constant of the VCMD model from (12) and is equal with $\frac{1}{k_v}$. From (26) and (27) the $K_{d_i}$ can be computed by:

$$ K_{d_i} = \frac{\frac{1}{\omega_{cg}^{\mu_i}}\tan\left[\varphi_m + \tan^{-1}(\omega_{cg}\tau) - \frac{\mu_i\pi}{2} + \pi\right]}{\cos\frac{(1-\mu_i)\pi}{2} - \frac{1}{\omega_{cg}^{\mu_i}}\sin\frac{(1-\mu_i)\pi}{2}}. \quad (28) $$

Using the derivative of the phase of the open loop system with respect to the frequency, the gain parameter $K_{d_i}$ is:

$$ K_{d_i} = \frac{-B \pm \sqrt{B^2 - 4A^2\omega_{cg}^{2\mu_i}}}{2A\omega_{cg}^{2\mu_i}}, \quad (29) $$

where $A = \frac{\tau}{1+(\omega_{cg}\tau)^2}$, $B = 2A\omega_{cg}^{\mu_i}\sin\frac{(1-\mu_i)\pi}{2} - \mu_i\omega_{cg}^{\mu_i-1}\cos\frac{(1-\mu_i)\pi}{2}$. Given the gain crossover frequency $\omega_{cg}$ and the desired phase margin $\varphi_m$, the parameters $K_{d_i}$ and $\mu_i$ are computed as a solution of equations (28) and (29). Thus, the parameter $K_{p_i}$ can be computed by:

$$ K_{p_i} = \frac{\omega_{cg}\sqrt{1+(\omega_{cg}\tau)^2}}{\sqrt{(1+K_{d_i}\omega_{cg}^{\mu_i}\cos\frac{\mu_i\pi}{2})^2 + K_{d_i}\omega_{cg}^{\mu_i}\sin\frac{\mu_i\pi}{2})^2}}. \quad (30) $$

Starting from classical control approach defined by (14), the proposed fractional order visual control law is given by:

$$ \mathbf{v}_c^* = -K_pG^{-1}(z^{-1})L_f^+(e + K_d\widehat{D}_k^{\mu}e), \quad (31) $$

where $K_p = [K_{p_1}...K_{p_i}]$ and $K_d = [K_{d_1}...K_{d_i}]$. In (31), $\widehat{D}_k^{\mu}e$ represent the estimated value of the fractional derivative from (23) at the sampling time $t_k = kT$:

$$ \widehat{D}_{kT}^{\mu}e = \frac{1}{T^{\mu}}\sum_{l=0}^{k}(-1)^l\begin{pmatrix}\mu\\ l\end{pmatrix}e(t-lT), \quad (32) $$

where $k = 0, 1, 2, ...$ and $T$ is the sampling period.

## IV. Control architecture

The proposed control approach for IBVS is evaluated through the visual servoing of a 6 d.o.f. manipulator with an eye-in-hand camera configuration. Thus, a simulator was developed and a high number of experiments were conducted and the obtained results were analyzed. The simulator illustrated in Fig.2 was constructed starting from an existing toolbox proposed in [17].

### A. Visual Control architecture

Planar objects are defined using points in Cartesian space. The blocks 'Initial position' and 'Desired configuration' are used to represent the start position $P_b(0)$ and the desired position $P_b^*$ of the object. Considering the frames attached to the robot base $F_b$, to the camera $F_c$ and to the object $F_o$, the homogeneous matrices $T_c^b$ and $T_o^b$ between the frames $F_c$ and $F_b$ and, respectively $F_o$ and $F_b$ are given. Knowing the position of the desired points related to the robot $P_b^*$ and the camera position related to the robot $T_b^c(0)$, the points position $P_c^*$, can be detected relatively to the camera coordinate system $F_c$ by using a homogeneous transformation implemented with 'Homog1' block. By a similar procedure, the initial position $P_b(0)$, respectively the current positions of the points are transposed from $F_b$ to $F_c$ frames using 'Homog2' block, resulting the initial/current position of the object points in the camera frame. The image of the object described by points given in Cartesian space is built using 'Perspective projection' blocks. For visualization of the object points in the image plane, the 'Camera view' block from Fig. 2 is employed.

Using the desired point features $f^*$ and current ones $f(k)$, the interaction matrices $L_f^*$ and $L_f(k)$ are computed employing (8) and (9). For better performances of the visual control law, the interaction matrix $L_f(k)$ can be replaced by $\widehat{LL} = 1/2\left(L_f^* + L_f(k)\right)$.

The 'Fractional Order Controller' block implements (31) and computes the command $\mathbf{v}_c^*(k)$ which represents the reference camera velocity. This signal is the input of the

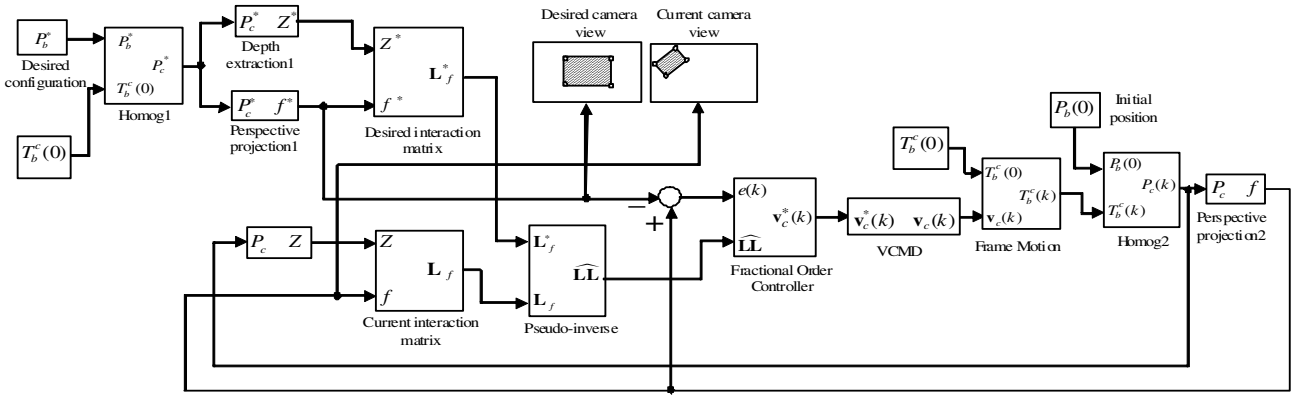


Fig. 2. Control architecture for visual servoing manipulator robot

VCMD model described by (13). The real camera velocity $\mathbf{v}_c$ is the output of the 'VCMD' block. Using screw velocity $\mathbf{v}_c$ and knowing the camera position related to the robot $T_b^c(0)$, the 'Frame Motion' block computes the new position and orientation of the camera $T_b^c(k)$ [17]. Assuming that the starting object features position related to the robot base $P_b(0)$ are known and using the camera pose stored in $T_b^c(k)$, the current point features coordinates are obtained.

### B. Simulation Results

The visual control strategy based on fractional order controller proposed in our paper was implemented, tested and fully validated in simulations. The proposed control architecture from Fig. 2 was implemented in Matlab for a planar object defined by 4 points in Cartesian space. Considering the visual servoing task configuration from Fig. 3, an image-based fractional order controller was designed and the conducted experiments revealed. The desired configuration is illustrated with red squares and the initial configuration is represented with blue circles, while the projection plane is marked with yellow.

The following points value from Cartesian space were considered:

$$\begin{aligned}\mathbf{X}_1 &= [0.25 \quad -0.25 \quad 0.14] \; \mathbf{X}_2 = [-0.25 \quad 0.23 \quad 0.14] \\ \mathbf{X}_3 &= [0.25 \quad 0.27 \quad 0.14] \; \mathbf{X}_4 = [-0.25 \quad -0.55 \quad 0.14]\end{aligned}. \tag{33}$$

Applying a perspective projection to the points from Cartesian space and using the initial and desired camera pose, the following point features are obtained:

$$\begin{aligned}f_1(0) &= [-0.11 \quad 0.27]^T; \quad f_2(0) = [-0.48 \quad 0.32]^T; \\ f_3(0) &= [-0.29 \quad 0.46]^T; \quad f_4(0) = [-0.16 \quad 0.01]^T; \\ f_1^* &= [0.22 \quad -0.13]^T; \quad f_2^* = [-0.22 \quad 0.29]^T; \\ f_3^* &= [0.22 \quad 0.32]^T; \quad f_4^* = [-0.22 \quad -0.40]^T;\end{aligned} \tag{34}$$

Assuming that the VCMD model (12) was designed as a diagonal matrix with equal value, $k_v = 160$, the sampling period $T$ must be at least $\frac{4}{k_v}$. All the experimental results from this paper were done considering $T = 1s$. The intrinsic camera parameters $p_x = p_y = 1000$ were chosen.

The gain crossover frequency and the phase margin are set as $\omega_{cg} = 65rad/s$, $\varphi_m = 74^o$. Thus, the optimum parameters for this servoing application of the image based fractional order controller are tuned [16] with the following values $K_p = 0.15$, $K_d = 0.056$ and the fractional order $\mu = 0.81$. The integer order $PD$ controller is obtained when $\mu = 1$. The tuning parameters for the classical $PD$ control were set as $K_p = 0.17$ and $K_d = 0.061$.

The image plane feature points trajectory is depicted in (Fig. 4(a), 4(b)). The performances of the classical $PD$ control and fractional $PD^\mu$ control is compared in Figs. 5 and 6 respectively. The camera velocity vectors are presented in Fig. 5. As can be observed, a fast convergence is obtained for the proposed image based fractional controller Figs. 5(a) and 5(b), whereas a slowest one is for classical approach Figs. 5(c) and 5(d). The number of iterations necessary

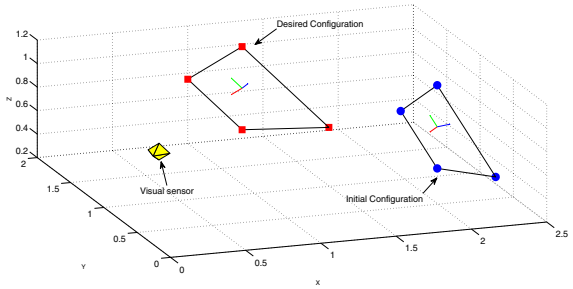


Fig. 3. Task configuration of servoing system

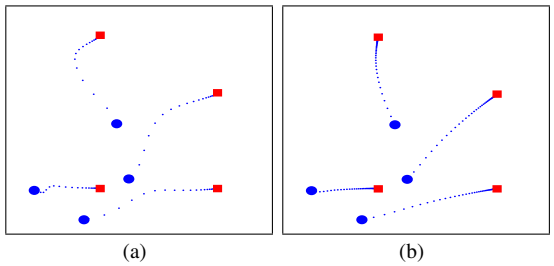

(a) (b)

Fig. 4. Image plane point features trajectory: (a) FO $PD^\mu$ controller; (b) classical $PD$ controller

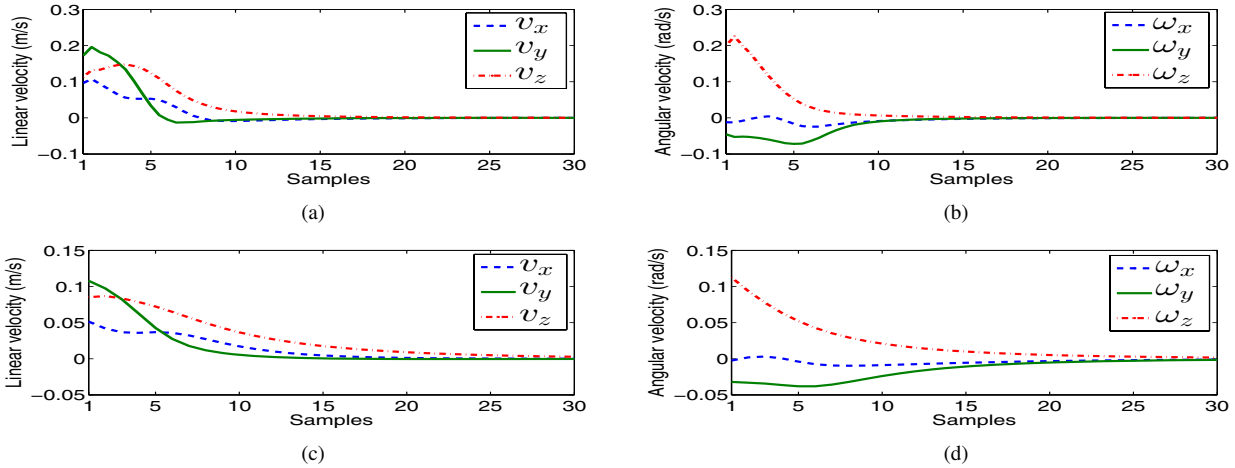


Fig. 5. The evolution of the linear and angular camera velocity for $FOPD^{\mu}$ approach (up) and classical $PD$ approach (down): (a) the linear velocity - $FOPD^{\mu}$; (b) the angular velocity - $FOPD^{\mu}$; (c) the linear velocity - $PD$; (d) the angular velocity - $PD$

to fulfill the visual servoing task is higher when classical controller is used than the number of iterations obtained when fractional controller is considered.

Computing the area of the point features error (Fig. 6) for the considered visual servoing application, the next values were obtained 15.649 and 22.462 for the $FOPD^{\mu}$ controller and $PD$ controller, respectively. The experimental results show a smaller error when the fractional order approach is used than the error obtained with the integer $PD$ controller. All the simulation results showed an improvement of the servoing system performances when dealing with proposed image based fractional order control law in comparison with the classical one. This results will dictate the possibility of a future implementation on a real servoing system and also, due the property of image moment features, to design a fractional order control law based on image moments.


Fig. 6. Point features error: (a) FO controller; (b) classical controller

## V. CONCLUSIONS

In this paper a visual servoing architecture for controlling an eye-in-hand 6 d.o.f. manipulator robot and a visual sensor is presented. The proposed control architecture uses fractional order approach and point features in order to design an image based control law. To evaluate the performances of the proposed fractional order controller, a simulator was developed and different simulation tests were considered. The best performances are obtained when the image based fractional order control law is considered in comparison with the classical one. As future work, the authors intend to apply this control approach on real servoing systems.

## REFERENCES


[1] O. Barambones and V. Etxebarria, "Robust neural control for robotic manipulator," *Automatica*, vol. 38, pp. 235–242, 2002.

[2] M. Llama, R. Kelly, and V. Santibanez, "Stable computed-torque control of robot manipulators via fuzzy self-tuning," *IEEE Trans. Syst. Man Cybern.*, vol. 30, pp. 143–150, 2000.

[3] E. Cruz and A. Morris, "Fuzzy-ga-based trajectory planner for robot manipulators sharing a common workspace," *IEEE Transaction on Robotics*, vol. 22, pp. 613–624, 2006.

[4] F. Chaumette and S. Hutchinson, "Visual servo control, part i: Basic approaches," *IEEE Robotics and Automation Magazine*, vol. 13, no. 4, pp. 82–90, 2006.

[5] M. Silva and T. Machado, "Fractional order pd$^{\alpha}$ joint control of legged robots," *Vibration and Control*, vol. 12, no. 12, pp. 1483–1501, 2006.

[6] J. Villagra, B. Vinagre, and I. Tejado, "Data-driven fractional pid control: application to dc motors in flexible joints," in *IFAC Conference on Advances in PID Control*, 2012.

[7] L. Cuvillon, L. Edouard, J. Gangloff, and M. de Mathelin, "Gpc versus h$\infty$ control for fast visual servoing of a medical manipulator including flexibilities," in *Proc. IEEE Int. Conf. on Robotics and Automation*, 2005, pp. 4044–4049.

[8] K. Hashimoto, T. Ebine, and H. Kimura, "Visual servoing with hand-eye manipulator-optimal control approach," *IEEE Trans. on Robotics and Automation*, vol. 12, pp. 766–774, 1996.

[9] J. A. Gangloff and M. F. de Mathelin, "High speed visual servoing of a 6 dof manipulator using multivariable predictive control," *Advanced Robotics*, vol. 17, no. 10, pp. 993–1021, 2003.

[10] S. Hutchinson, C. Hagerand, and P. Corke, "A tutorial on visual servo control," *IEEE Trans. On Robotics and Automation*, vol. 12, no. 5, pp. 651–670, 1996.

[11] H. Fujimoto, "Visual servoing of 6 dof manipulator by multirate control with depth identification," in *Proc. of 42 nd IEEE Conference on Decision and Control*, Hawaii, 2003, pp. 5408–5413.

[12] G. Allibert, E. Courtial, and F. Chaumette, *Visual servoing via Advan. Numer. Methods*. Springer, 2010, ch. Visual servoing via nonlinear predictive control, pp. 375–393.

[13] T. Murao, T. Yamada, and M. Fujita, "Predictive visual feedback control with eye-in-hand system via stabilizing receding horizon approach," in *Proc. of 45th IEEE CDC*, 2006, pp. 1756–1763.

[14] C. Copot, C. Lazar, and A. Burlacu, "Predictive control of nonlinear visual servoing systems using image moments," *IET Control Theory and Applications*, vol. 6, no. 10, pp. 1486–1496, 2012.

[15] N. Mansard, A. Remazeilles, and F. Chaumette, "Continuity of varying-feature-set control laws," *IEEE Trans. on Automatic Control*, vol. 54, no. 11, pp. 2493–2505, nov 2009.

[16] C. Monje, Y. Chen, B. Vinagre, D. Xue, and V. Feliu, *Fractional-order Systems and Controls. Fundamentals and Applications*. Springer, 2010.

[17] E. Cervera, "Visual servoing toolbox," http://vstoolbox.sourceforge.net/, Castellon, 2003, Jaume I University.